



Toxicity and Neuroendocrine Regulation of the Immune Response: A Model Analysis

E. MURAILLE†¶, D. THIEFFRY‡, O. LEO† AND M. KAUFMAN§

† *Laboratoire de Physiologie Animale and ‡ Laboratoire de Génétique des Procaryotes, Université Libre de Bruxelles, Rue des chevaux, 67, B-1640 Rhode Saint Genèse, and the § Centre for Nonlinear Phenomena and Complex Systems, Université Libre de Bruxelles, Campus Plaine C.P.231, B-1050 Bruxelles, Belgium*

(Received on 18 August 1995, Accepted in revised form on 11 July 1996)

Various models have been proposed for the regulation of the primary immune response. Most of these models focus on the ability of the immune system to control a multiplying pathogen, and take into account the cross-regulations between different immune components. In the present study, we integrate the immune system in the general physiology of the host and consider the interaction between the immune and neuroendocrine systems. In addition to pathogen growth and toxicity, our four-variable model takes into account the toxic consequences for the organism of the immune response itself, as well as a neuro-hormonal retro-control of this immune response.

Formally, the dynamics of the model is first explored on the basis of a discrete caricature, with special emphasis on the role of the constitutive feedback loops for determining the essential dynamical behavior of the system. This logical analysis is then completed by a classical continuous approach using differential equations.

From a biological point of view, our model accounts for four stable regimes which can be described as “pathogen elimination/organism healthy”, “pathogen elimination/organism death”, “pathogen growth/organism death” and “chronic infection”. The size of the basins of attraction of these different regimes varies as a function of some crucial parameters. Our model allows moreover to interpret the interplay between pathogen immunogenicity and neuro-hormonal feedback, the effects of stress on immunity and the toxic shock syndrome, in terms of transitions among the steady states.

© 1996 Academic Press Limited

1. Introduction

Several models have been proposed for the regulation of the specific (Fishman & Perelson, 1993) and innate (Antia & Koella, 1994) immune response. These models focus on the ability of the immune system to respond to a replicating pathogen and failure to control pathogen growth is interpreted as leading to the death of the host (De Boer & Hogeweg, 1986; Schweitzer & Anderson, 1991; McLean & Nowak, 1992; Behn *et al.*, 1993; Brass *et al.*, 1994; Fishman & Perelson, 1994; De Boer & Perelson, 1995). In the context of these studies, negative feedbacks on the

immune system account for the termination of the immune response and for self-tolerance. Here, we present a model which is centered on the coupling between the immune, nervous and endocrine systems. This model takes into account the damages inflicted by the pathogen to the organism as well as the toxicity of the immune response itself. It is based on the following immunological observations, summarized in Fig. 1.

(1) In numerous diseases, harmful or lethal effects for the organism are mostly due to the immune response rather than directly to pathogen toxicity. For example, evidence is accumulating that the pathology observed in cerebral malaria is not directly caused by Plasmodium products but by excessive

¶ Author to whom correspondence should be addressed.
E-mail: emura@ulb.ac.be

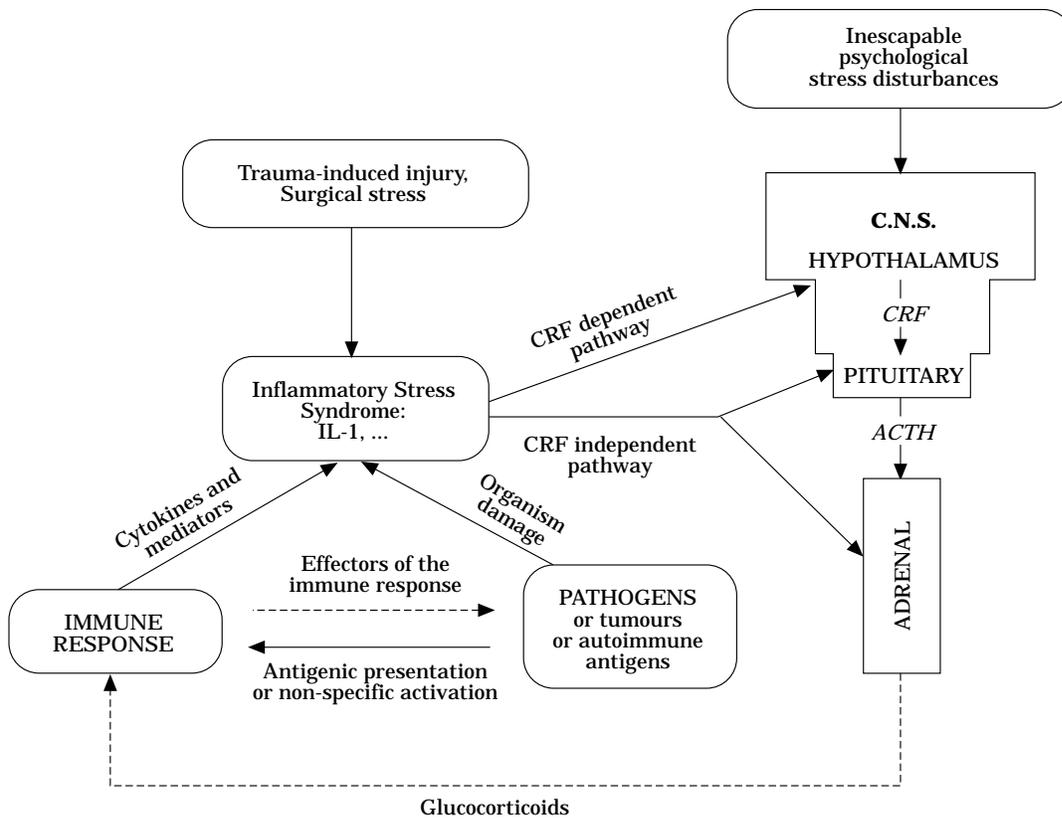


FIG. 1. Schematic representation of the neuro-endocrine control of the immune response. Solid arrows indicate stimulatory interactions and dashed arrows correspond to inhibitory interactions.

concentrations of normal components of the immune response, mainly cytokines such as interferon- γ (IFN- γ) and tumour necrosis factor α (TNF- α) (Karunaweera *et al.*, 1992; de-Kossodo & Grau, 1993). Similarly, it is widely believed that hepatic damage associated with hepatitis-A (Fleicher *et al.*, 1990) and -B (Ando *et al.*, 1993) virus infections are induced by an immunopathological reaction of sensitized cytotoxic T cells against infected hepatocytes. Overwhelming bacterial infections are accompanied by a Systemic Inflammatory Response Syndrome (SIRS) and a Multiple Organ Dysfunction Syndrome (MODS) leading to death. Many studies have shown that these symptoms are caused by the TNF- α cytokine, produced in response to endotoxins (LPS) and superantigens (Miethke *et al.*, 1992) released by the bacteria. Thus, pathogens weakly toxic by themselves may trigger the release of host toxic products. Let us stress that low concentrations of these cytokines are, in most cases, not only harmless but necessary for normal biological functions. They become deleterious when over- or chronically produced. To account both for the injuries caused by the pathogen to the host and the pathological consequences of immune responses, we

consider explicitly the health state of the organism in our modeling (see also Marchuk *et al.*, 1991; Bocharov & Romanyukha, 1994).

(2) The neuroendocrine system has well-demonstrated effects on immune functions. The interplay between these two physiological systems is most commonly associated with the pronounced effects of stress on immunity. The hypothalamo-pituitary-adrenocortical (HPA) axis is a key player in stress responses and its activation represents a major adaptive response to stressful circumstances such as infections, psychological disturbances, trauma-induced injuries and surgical stress. The pro-inflammatory interleukin-1 (IL-1), produced by many activated immune cells, keratinocytes and endothelial cells (for a review see Titus *et al.*, 1991), has been identified as an important activator of the HPA response *in vivo* (Sapolsky *et al.*, 1987). This cytokine stimulates the release of Corticotropin-Releasing Factor (CRF) by the hypothalamus, leading to the production of AdrenoCorticoTropic Hormone (ACTH) by the pituitary. ACTH in turn induces the release of glucocorticoids by the adrenal glands. It has been shown that glucocorticoids may act as an immunosuppressive and anti-inflammatory agent to

lower life threatening reactions of the immune system (Kunicka *et al.*, 1993; Gonzalo *et al.*, 1993; Brown *et al.*, 1993; Dobbs *et al.*, 1993). These data suggest that the brain is able to monitor the progress of immune responses. As a consequence of its pivotal role in the immune-neuroendocrine interactions the HPA axis is a main component of our approach.

The complex graph presented in Fig. 1 has been simplified into a four-element model. Each of these elements represents, in a global way, a family of actors of the system: the first element is the pathogen or antigen level; the second element represents the size of the immune response, e.g. the numbers of activated immune effectors and cytokine and immunoglobulin concentrations; the third element characterizes the health state or viability of the organism and reflects the degree of damages of target organs and vital functions; finally, the fourth element describes the neuroendocrine HPA component and corresponds, in particular, to the concentration of circulating glucocorticoids. The graph of interactions corresponding to our model is presented in Fig. 2(a).

The paper is organized as follows. In the next section, we present our four-variable differential model and discuss its main components. In the third section, we introduce a logical approach and describe the logical caricature of our differential model. In the fourth section, the main results of our model analysis are presented and discussed, both from a dynamical and biological point of view. The last section is devoted to concluding remarks and perspectives.

2. A Four-Variable Differential Model

The basic interactions of our model [Fig. 2(a)] are:

- (1) the proliferating pathogen stimulates the immune response and negatively affects the viability of the organism;
- (2) the immune response neutralizes the pathogen and is harmful for the organism. It also activates the HPA axis;
- (3) the HPA axis, in turn, downregulates the immune response.
- (4) the organism ensures its own maintenance and is necessary for the occurrence of an immune response. Formally, these interactions are described by the following set of dimensionless differential equations:

$$dP/dt = P\{[k_p P/(1 + P)] - [1 + k_i R]\} \quad (1)$$

$$dR/dt = k_r FA_1 FA_3 FI_4 - d_r R \quad (2)$$

$$dO/dt = k_o FA_3 - O[d_o + \alpha P + \beta R] \quad (3)$$

$$dH/dt = k_h FA_2 - d_h H \quad (4)$$

in which P , R , O , and H represent, respectively, the concentration of pathogen ($k_p > 0$) or nonproliferating antigen ($k_p = 0$), the level of immune response, the "health" of the organism and the global level of hormonal control.

The detailed mechanisms of antigen presentation, cytokine regulation and organism maintenance are not described. These maintenance, stimulatory or inhibitory processes are represented, globally, by the increasing sigmoids $FA_1 = P^2/(s^2 + P^2)$, $FA_2 = R^2/(1 + R^2)$, $FA_3 = O^2/(1 + O^2)$, and by the decreasing sigmoid $FI_4 = 1/(1 + H^2)$. These nonlinear functions express the fact that those interactions which have a

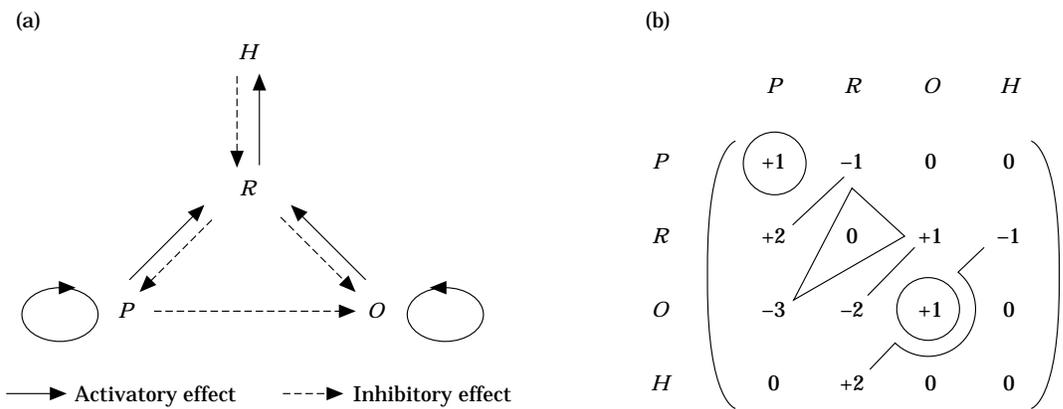


FIG. 2. (a) Graph and (b) matrix of interactions for our four variable model, P , R , O and H represent, respectively, the level of the pathogen, the size of the immune response, the state of the organism and the level of the neuroendocrine feedback. In the matrix, the signs and the numbers correspond to the signs and the thresholds of the different interactions; for example, -2 in row 3/column 2 means that R exerts a negative effect on O above its second threshold. The feedback loops of the system are indicated by circles (one-element loops) and lines. We use a four-valued logical variable for the pathogen (P), a three-valued logical variable for the immune response (R) and a one-valued variable for the organism state (O) and the HPA hormonal axis (H).

regulatory character are, most often in biology, doubly nonlinear: there is a “threshold” concentration below which the regulator is inefficient and a boundary value of its effect. On the other hand, the pathogen is removed by the immune system at a rate proportional to the size of the immune response. Similarly, destruction of the target organ cells and vital functions of the organism occurs at a rate proportional to the pathogen load or level of immune response. In each of the four equations, a linear term accounts moreover for the spontaneous and non-specific decay of the corresponding variable.

In eqns (1–4) each concentration variable has been scaled by its threshold value. The pathogen concentration has been scaled by its lowest, proliferation, threshold, and time by the pathogen death rate d_p ($1/d_p$: pathogen life expectancy). The parameters in these equations are thus composite parameters given explicitly in appendix C.

In eqn (1), the proliferation term, $P[k_p P/(1 + P)]$, contains a lower threshold and accounts for a density dependent proliferation rate; this means that, at extremely low pathogen densities, the pathogen can be considered as extinct. The second term, $P[1 + k_i R]$, describes non-specific and immune dependent pathogen removal. It should be stressed that the trivial state, corresponding to pathogen elimination, is always a stable steady state.

In eqn (2), the first term, $k_r FA_1 FA_3 FI_4$, combines three contributions. FA_1 and FA_3 account for the usual conditions to evoke an immune response, i.e. the presence of antigen at a sufficient concentration ($FA_1 \approx 1$) and an healthy organism ($FA_3 \approx 1$). The third (decreasing) sigmoid, FI_4 , represents the inhibitory effect of the HPA axis on the immune response. Note that as long as the organism remains viable immunocompetence is here only slightly affected by the state of the organism. Specific immunosuppression associated with a particular type of infection is not considered at this stage.

In eqn (3), $k_o FA_3$ accounts for the fact that an organism in very “bad shape”, will decline and die (lower branch of the sigmoid), whereas an organism in “good shape” promotes its own maintenance (upper branch of the sigmoid). Pronounced destruction of target and vital organs such as for instance the airways, liver or heart, corresponds to greatly decreased values of O and are lethal ($O = 0$).

In eqn (4), the activatory effect of the immune system on the HPA axis is represented by an increasing sigmoid, FA_2 , to take into account the existence of an activation threshold as found by Sternzel-Poore *et al.* (1993).

A series of parameters qualitatively describe the pathogen and host characteristics:

— k_p gives an estimation of the pathogen proliferation rate;

— k_r globally quantifies the immunogenic properties of the pathogen and the corresponding immune system reactivity related, for example, to host genetic background and nutritional status, environmental factors or presence of concomitant infections;

— k_i represents the sensitivity of the pathogen to the immune response;

— α gives a measure of the level of toxicity of the pathogen for the organism, i.e. the damages inflicted by the pathogen itself.

— β represents the toxicity, for the organism, of the immune response that is induced by the pathogen; note that, depending on the site of pathogen proliferation, the same immune response may be more or less injurious.

— k_h characterizes the responsiveness of the neuroendocrine system to inflammatory immune mediators, depending on several factors such as the pathway of interaction or antecedents of the organism; this parameter may also reflect the presence of glucocorticoid antagonists in the circulation.

In addition to the classical aspects of an immune response, i.e. control and elimination of the pathogen, chronicity and latent infection, killing of the organism by the pathogen when the immune response does not succeed in controlling pathogen growth, this set of parameters allows to consider different pathogen profiles and special immune situations, such as toxic shock and stress effects.

Clearly, our differential system comprises multiple intertwined feedback loops. In order to localise all its steady states and to get a qualitative insight in its main dynamical features, we first analyse a “logical caricature” of the system.

3. Logical Approach

3.1. LOGICAL BACKGROUND

Thomas and collaborators have recently developed logical tools for the analysis of complex regulatory networks (Thomas & D’Ari, 1990; Thomas, 1991). Their method focuses on the dynamical role of regulatory circuits called feedback loops. In short, a feedback loop is any closed series of interactions where each element appears only once (“oriented circuit” in the language of Graph Theory). All feedback loops can be classified into positive or negative, according to whether they have an even

or an odd number of negative interactions. These two types of loops have strikingly different dynamical properties: positive loops can generate multistationarity, whereas negative loops can generate homeostasis.

Formally, the elements of a network and the interactions between them are represented by discrete variables, functions, and parameters. In the simplest cases, these take only two values (zero or one). However, when modeling complex regulatory systems where some variables have several distinct actions, one often needs to account for more than two qualitatively different levels for some of the variables. Accordingly, when necessary, one uses logical variables endowed with more than two values. Moreover, one also considers explicitly the threshold values separating the regular logical values. For a multi-level logical variable (and its corresponding function and parameters), one has thus a limited set of possible values of the type $\{0, s^{(1)}, 1, s^{(2)}, 2, \dots\}$ where $s^{(i)}$ represents the threshold separating values zero and one, etc.

This formalism leads to a limited number of combinations of the variable values, each corresponding to a different state of the system. Among these combinations, some involve only regular values and are thus called “regular states”, whereas others involve one or more threshold values and are called “singular states”.

Recently, Thomas and collaborators have proposed that each feedback loop can be characterized by a singular logical state located on the thresholds at which the variables act in the loop (Snoussi & Thomas, 1993; Thomas *et al.*, 1995). For proper parameter values, this characteristic state is steady in the *subspace* of the variables of the loop and the corresponding loop is functional. “Functional” means that if the loop is positive, it actually produces multistationarity (and the characteristic state is located on the separatrix between the two attractors of the system); if the loop is negative, it generates homeostasis, i.e., the variables of the loop tend to middle range values, with or without oscillations. This notion of loop-characteristic state can be generalized to include states characteristic of sets of loops (Thomas *et al.*, 1995).

In the context of this “generalized logical description”, one can easily compute the parameter constraints to render a given feedback loop functional. Moreover, comparing different sets of parameter constraints, one can check if any group of loops may be functional simultaneously. The analysis of the behavior of a network thus boils down to dissociating the network into its constituent

feedback loops and checking their dynamical role, yet keeping full control on the way in which the loops are interconnected.

The correspondence between logical and differential parameter constraints becomes perfect as one uses steeper and steeper Hill functions to represent the interactions between the variables. More specifically, in the case of a simple, functional, positive loop, one finds an unstable steady state located at or near the threshold values (a saddle point for a two variable system) and two attractors which are stable nodes. In the case of a negative loop, one also finds a steady state located at or near the threshold values, but it may be stable or unstable (stable fixed point for 1-variable, stable focus for 2-variable, and a stable or unstable steady state with a periodic component for 3-variable systems). Thus, in the differential description as in the logical description, we can associate a characteristic state with each simple feedback loop, the steadiness of this characteristic state expressing the functionality of the corresponding loop.

Dealing with a complex network, we show in this paper that what can be learned about the dynamical role of individual feedback loops in the logical context can be extended to homologous differential models.

3.2. A LOGICAL CARICATURE OF OUR FOUR-VARIABLE DIFFERENTIAL MODEL

From the graph of interactions [Fig. 2(a)], we derive the “matrix of interactions” shown in Fig. 2(b). The $+/-$ signs and numbers denote the stimulatory or inhibitory nature of the interactions and their corresponding threshold, respectively; for example, -2 in row 3/column 2 means that R exerts a negative effect on O above its second threshold. Note that we use a four-valued logical variable for the pathogen (P), a three-valued logical variable for the immune response (R) and two-valued variables for the organism (O) and the HPA hormonal axis (H). The feedback loops of the system are indicated by circles (one-element loops) and lines. One can easily localise six feedback loops, including three positive and three negative loops, which may be labelled **P**, **O**, **POR** and **PR**, **RO**, **RH**, respectively.

Using a computer program (Thieffry *et al.*, 1993), the parameter constraints for which each of the six feedback loops is functional can easily be determined. In fact, one can find constraints such that all six feedback loops are functional simultaneously, at least in their respective subspace (see Appendix A).

On the basis of biological considerations, we have chosen a specific set of values for the logical parameters which is consistent with the constraints imposing that all six feedback loops are functional,

TABLE 1
Loop functionality, logical and differential steady states [P, R, O, H]

Loops	Signs	Functionality domains	Logical steady states	Differential steady states	Stability
P	+	$s^{(1)}[0][01][01]$	$[s^{(1)}000]$	[0.17, 0, 0, 0]	Unstable
O	+	$[012][01]s^{(1)}[01]$	$[s^{(1)}010]$	[0.19, 2.94 10^{-3} , 2.34, 1.73 10^{-4}]	Unstable
PR	-	$s^{(2)}s^{(1)}[1][0]$	$[00s^{(1)}0]$	[0, 0, 0.42, 0]	Unstable
RO	-	$[2]s^{(2)}s^{(1)}[0]$	$[s^{(2)}s^{(1)}10]$	[1.02, 7.44 10^{-2} , 1.63, 0.11]	Stable
RH	-	$[23]s^{(2)}[1]s^{(1)}$	-	-	-
POR	+	$s^{(3)}s^{(1)}s^{(1)}[0]$	$[s^{(3)}s^{(1)}s^{(1)}0]$	-	-
P*O	+ * +		$[s^{(1)}0s^{(1)}0]$	[0.17, 4.34 10^{-4} , 0.42, 3.77 10^{-6}]	Unstable
PR*O	- * +		$[s^{(2)}s^{(1)}s^{(1)}0]$	[1.73, 0.10, 0.77, 0.20]	Unstable
			[0000]	[0, 0, 0, 0]	Stable
			[3000]	unbound exponential growth of the pathogen	
			[0010]	[0, 0, 2.38, 0]	Stable

The first two columns contain the different feedback loops of the system and their corresponding sign. For each of these loops, the third column gives the domains of functionality for the parameter values chosen (see Table A1). The fourth column indicates the corresponding singular steady states, plus the three regular steady states of the system (three last rows). Finally, the last two columns give the continuous counterparts of the logical steady states and their stability, for the parameter values corresponding to Appendix C. Note that **P*O** and **PR*O** represent combinations of disjoint loops (i.e. loops which do not share any element) which generate a common characteristic state.

at least in a region of the variable space (see third column of Table 1 and Appendix A). In fact, these values amount to impose “AND” constraints wherever several interactions are exerted on a same element.

For parameter values consistent with these constraints, the system has ten steady states, three “regular” stable states, [0000] (zero state), [0010] (pathogen dead, organism alive) and [3000] (pathogen growing, organism dead), and seven “singular” steady states, i.e. states located on one or more thresholds, which are characteristic of loops **P**, **O**, **PR**, **POR** and of the union of loops **P*O** and **PR*O**. The logical values of these states are given in the fourth column of Table 1. Among these singular steady states only state $[s^{(2)}s^{(1)}10]$, the chronic infection state, characteristic of the negative loop **PR**, can be stable. All the other singular states are characteristic of (at least) one positive loop and are thus located on a separatrix and unstable.

4. Results and Discussion

4.1. STEADY STATES ANALYSIS

Let us now give a general view of the attractors and main dynamical properties of the differential model. The logical constraints which ensure the functionality of all six feedback loops have been used to derive reference values for the parameters of the differential equations.

Using the qualitative information derived from the logical analysis (number, nature and approximate location of the steady states), we have determined

the steady states in the differential description. We have first located the *stable* states by numerical integration of the differential eqns (1–4). This gives the continuous counterpart of the logical values at these steady states. These continuous values have been used to locate the *unstable* steady states by iteration. In addition, the differential steady states have been checked by the graphical and numerical resolution of a polynomial in *R* constructed from eqns (1–4), as shown in Appendix B.

The steady states corresponding to both the logical caricature and the differential model are given in Table 1. As seen in this table, eight of the ten steady states which are predicted by the logical analysis are also found in the differential system. Each of these steady states has a location, a nature (focus-saddle point, node, . . .) and a stability consistent with the logical predictions. More specifically, only the differential steady states corresponding to regular logical steady states, plus the steady state characteristic of the negative loop **PR**, $[s^{(2)}s^{(1)}10]$, are stable. As expected, this latter is periodically attractive. All the other differential steady states, corresponding to characteristic states of positive feedback loops are unstable.

The absence of differential steady states corresponding to the logical steady states [3000] and $[s^{(3)}s^{(1)}s^{(1)}0]$ can be explained without difficulty considering that the differential system involves an exponential (unbound) interaction which is represented by a (bound) threshold function in the logical caricature. Indeed, there is no upper bound to pathogen growth in the differential eqn (1). Thus, to the logical state [3000] corresponds simply an

TABLE 2
Biological interpretation of the attractors of the system

Differential attractors [<i>P</i> , <i>R</i> , <i>O</i> , <i>H</i>]	Immunological interpretation	Logical counterparts [<i>P</i> , <i>R</i> , <i>O</i> , <i>H</i>]
[0, 0, 0, 0]	pathogen elimination and organism death	[0, 0, 0, 0]
[0, 0, 2.38, 0]	healthy, uninfected organism	[0, 0, 1, 0]
[∞, 0, 0, 0]	unbound exponential growth of the pathogen	[3, 0, 0, 0]
[1.02, 7.44 10 ⁻² , 1.63, 0.11]	pathogen persistence	[<i>s</i> ⁽²⁾ , <i>s</i> ⁽¹⁾ , 1, 0]

The parameter values for the differential eqns (1–4) are here as defined in Appendix C. The parameter values chosen for the logical caricature are given in Table A1.

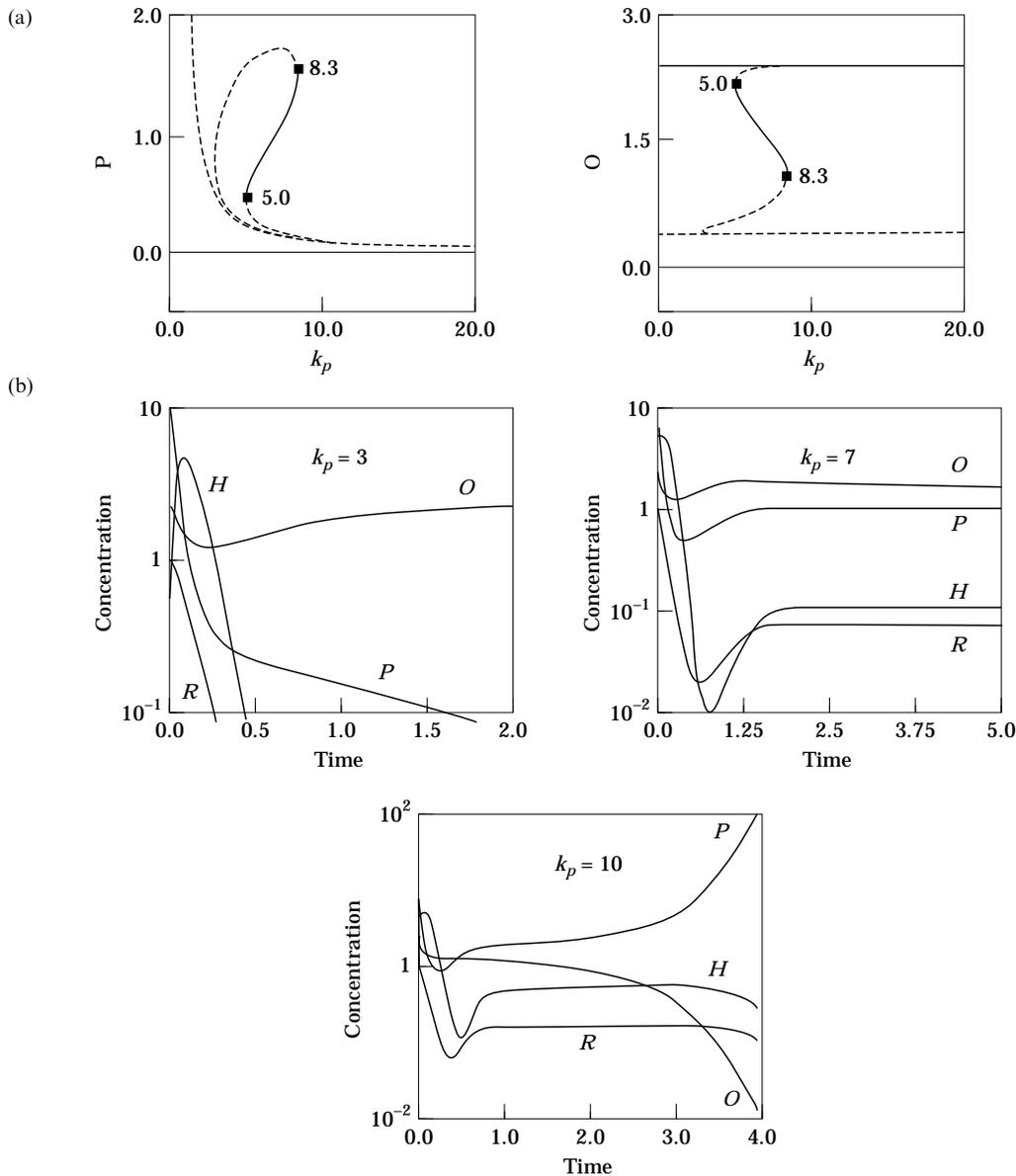


FIG. 3. (a) Bifurcation diagrams giving the steady state branches for the pathogen concentration, *P*, and the state of the organism, *O*, as a function of the pathogen growth rate *k_p*. Other parameter values are as in Appendix C. Solid lines correspond to stable branches, dashed lines to unstable branches. (b) Time evolution for different values of the pathogen growth rate *k_p*, and other parameter values as listed in Appendix C. The initial state corresponds to a healthy organism infected with a pathogen dose *P* = 10. *k_p* = 3: pathogen elimination is accompanied by full recovery of the organism. *k_p* = 7: pathogen growth is controlled but a state of chronic infection settles. *k_p* = 10: the immune response is too weak to control the growth of the pathogen; a long lasting immune response together with damages inflicted by the pathogen lead to organism death.

exponential growth of the pathogen in the differential description. As regards the second state, $[s^{(3)}s^{(1)}s^{(1)0}]$, characteristic of the positive loop **POR**, we know that in the logical formalism $s^{(3)}$ separates the lower values of P (0–2) from its top value (3). This top value is pushed towards infinity in the differential system and it is thus not surprising to lose the threshold value $s^{(3)}$ when we proceed from the logical to the differential description.

The physiological meaning of the four attractor states of the system is summarized in Table 2.

4.2. FEEDBACK LOOP ANALYSIS AND BIFURCATION GRAPHS

In Fig. 3(a), we present the bifurcation graphs corresponding to the pathogen level or state of the organism vs. pathogen growth rate (k_p). Depending on the value of k_p , the system may have from three up to eight steady states, with two to three stable states. Note that some bifurcation branches are degenerate and correspond to different steady states in the full variable

space, as illustrated in Table 1 for $k_p = 7$. A series of typical time plots for different values of k_p is given in Fig. 3(b) which illustrates three of the four possible regimes of the system, namely “pathogen death/organism recovery” [0010], “chronic state” $[s^{(2)}s^{(1)10}]$ and “pathogen growth/organism death” [3000].

The system contains several intertwined feedback loops and it is not straightforward to predict the effect of parameter changes in the differential system. However, this can be done very easily for the logical caricature. A systematic logical analysis of the constraints governing the functionality of the different loops of the system shows that most of the parameters are involved in the functionality of more than one loop (see Appendix A). To study the role of individual loops, we have looked for modifications of the logical parameters such that only one loop at a time loses its functionality. Two logical parameters have been selected. One corresponds to k_i , the strength of inhibition of the pathogen by the immune response, which controls the functionality

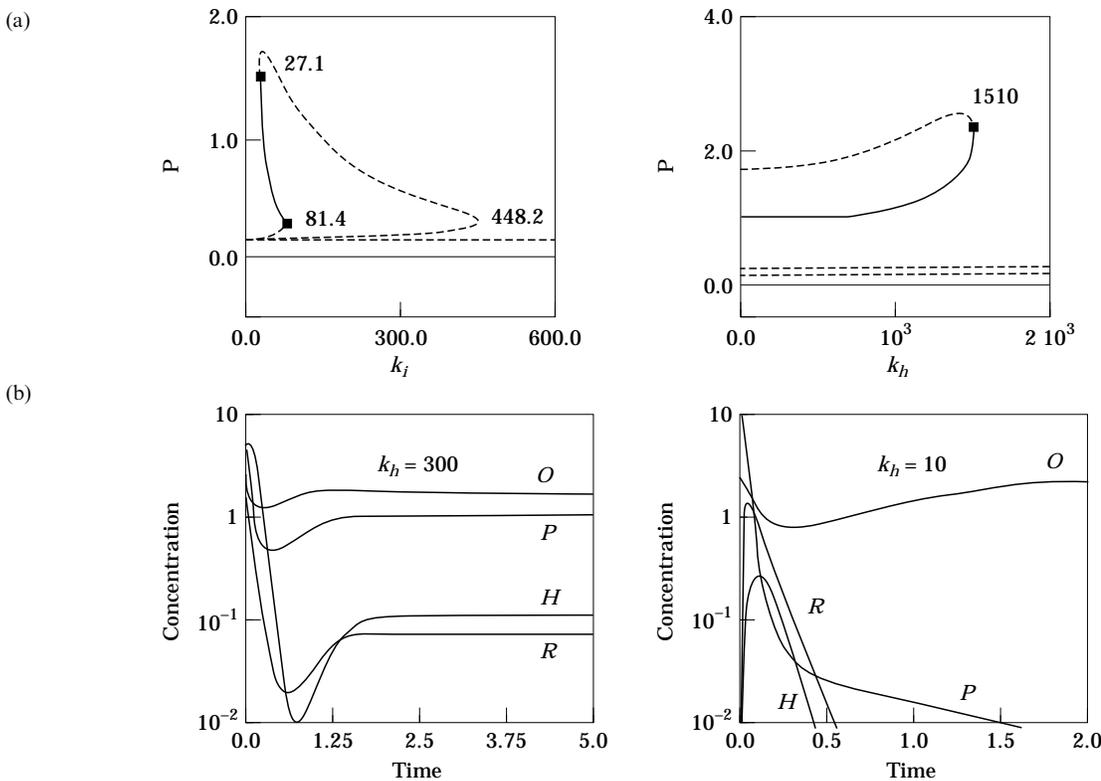


FIG. 4. (a) Bifurcation diagrams for the steady state concentrations of the pathogen as a function of the elimination rate of the pathogen by the immune response, k_i , and of the strength of activation of the neuroendocrine (HPA) axis, k_h . The other parameter values are given in Appendix C. Solid lines correspond to stable branches, dashed lines to unstable branches. In both cases there exists a region of multistationarity which includes a stable steady state corresponding to chronic infection. (b) Time evolution for different values of k_h , the strength of activation of the HPA axis. The initial state corresponds to a healthy organism infected with a pathogen dose $P = 10$. Depending on the strength of the negative feedback of the HPA axis on the immune response, one observes the establishment of the chronic infection state ($k_h = 300$) or the rapid elimination of the pathogen and full recovery of the organism ($k_h = 10$). The other parameter values are as in Appendix C.

of the one-variable positive loop **P**. The other corresponds to k_h , the strength of activation of the HPA axis by the immune response, which controls the functionality of the two-element negative loop **RH**.

Even though our differential model is not exactly homologous with its logical caricature, we expect that corresponding parameter modifications will produce qualitatively similar changes in the dynamics of both models. Thus, we predict that modifying k_i will affect the multistationarity properties of the systems, whereas modifying k_h will influence its homeostatic properties.

In Fig. 4, the bifurcation graphs corresponding to these two parameters are shown. One sees, in Fig. 4(a), that there is a limited range of k_i values allowing for multistationarity. At low k_i this range includes the chronic infection attractor $[s^{(2)}s^{(1)}10]$. On the other hand, there is a large range of k_h values (from 0 to ca. 1500) for which there are no changes in the number and stability of the steady states. Shown in Fig. 4(b) are two typical time plots obtained for medium and low values of k_h . Starting

with identical initial conditions, the system reaches the chronic attractor in the first case, whereas in the second case one observes full recovery of the organism. Thus, as expected from the logical analysis, the basin of attraction of the homeostatic state (chronic attractor) is considerably reduced as k_h decreases. It should be noted that for very high k_h the chronic attractor disappears. Considering the differential equations, one can see that high k_h values will lead to high H and low FI_4 . Since FI_4 enters a product of sigmoids in eqn (2), k_h affects indirectly the level of R , in the differential description, and tends to uncouple the equation for the pathogen.

The analysis of other parameter changes is more subtle. Indeed, the logical analysis predicts that all other parameters affect at least one positive and one negative loop (see Appendix A). Thus, changing any of these parameters should affect both the homeostatic and multistationarity properties of the system. Bifurcation graphs and typical time plots corresponding to some of these parameters are discussed in the next section.

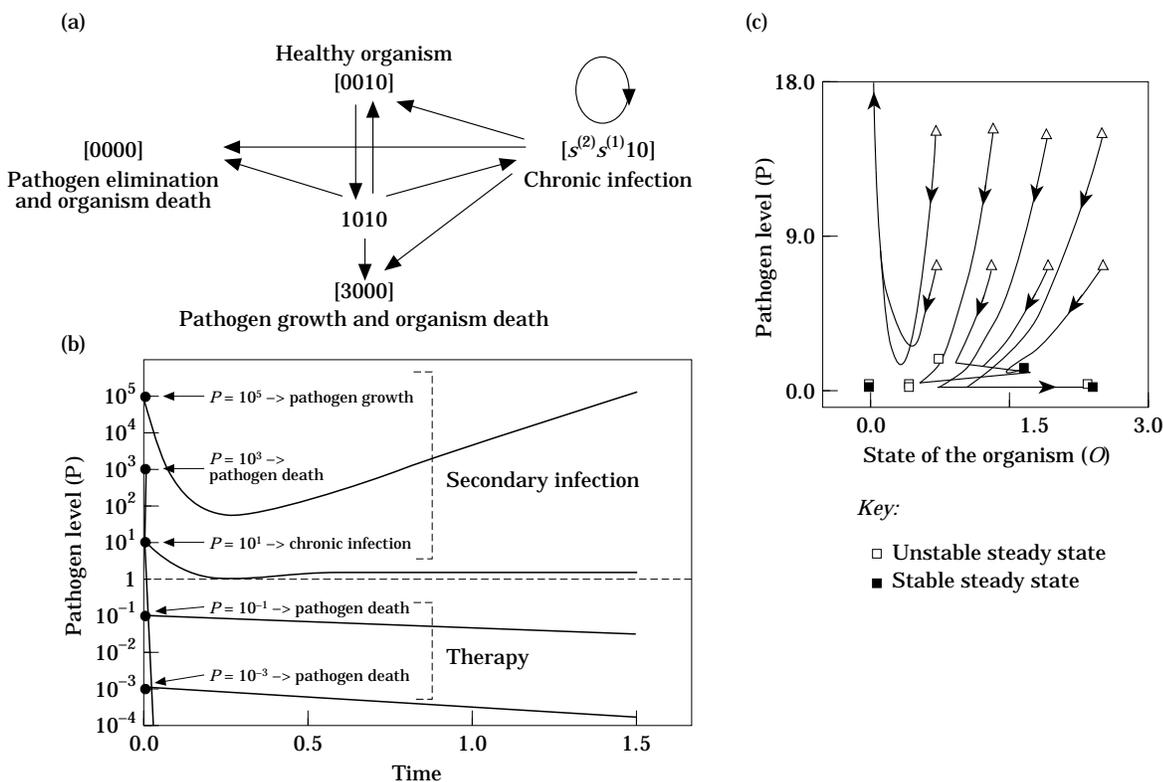


FIG. 5. Influence of the pathogen dose and the state of the organism on the outcome of infections. (a) Regime states and possible transitions upon pathogen encounter. (b) Influence of the addition or removal of pathogen on the evolution of a chronic infection. The system is initially in the chronic infection state $P = 1.18$, $R = 0.09$, $O = 1.46$, $H = 0.17$. At time $t = 0$, pathogen is added or removed and the system is then allowed to evolve freely. The parameters are as in Appendix C, except for $k_p = 8$ and $k_i = 36$. It can be seen that, within a given range of pathogen doses, secondary infections now lead to rapid pathogen elimination and full recovery of the organism. (c) Influence of the initial state of the organism (O) on the outcome of an infection, as a function of two different pathogen doses. At time $t = 0$, $R = H = 0$. The parameter values are those of Appendix C.

4.3. IMMUNOLOGICAL INTERPRETATIONS AND PREDICTIONS

4.3.1. Influence of the size of the infecting pathogen dose and the state of the organism on the outcome of infections

Figure 5(a) summarizes the possible transitions among the different regime states of our system. Starting from an healthy organism (steady state [0010]) infected by the pathogen (state 1010), the system may evolve toward any one of the four attractors described in the preceding sections, depending on the pathogen dose and parameter conditions. On the other hand, the steady state [$s^{(2)}s^{(1)}$]0] corresponding to a chronic infection can be destabilized by adding (secondary infection) or removing (therapeutical treatment) the pathogen. Figure 5(b) shows that starting from the chronic state, secondary infections or neutralization of the pathogen may lead the system to the states [3000], [0010] or back to the chronic infection state [$s^{(2)}s^{(1)}$]0]. It should be stressed that, within a given range of pathogen doses, secondary infections may be accompanied by pathogen elimination and full recovery of the organism.

In our model, the outcome of an infection also depends on the state of the organism (i.e. O level) upon pathogen encounter. As illustrated in Fig. 5(c) for a given set of parameters, an organism in good or relatively good shape is able to eliminate the pathogen or at least to master the pathogen growth, depending on the strength of the infection and initial state of the organism. On the contrary, an organism in bad shape will be pushed towards death with an exponential growth of the pathogen. This latter situation arises, for instance, if a second encounter with a pathogen occurs before the organism has significantly recovered from a first strong infection during which the pathogen has been eliminated.

Our model thus accounts for the fact that an organism will be more or less resistant to infection depending on its initial health condition and on the strength of the infection. It also suggests that addition of pathogen may cure persistent infections by boosting the response, as has also been predicted in some other models of immune regulation (Behn *et al.*, 1993; Segel & Jäger, 1994; Segel *et al.*, 1994).

4.3.2. Immunogenicity, toxicity and neuro-hormonal feedback

Classically, organism death following an infection is attributed to the failure of the immune system to master the pathogen, and the pathogen itself is considered as the main injury cause. In this

perspective, the problem of an adequate immune response is boiled down to the production of the strongest and the best fitted response to the infecting pathogen. Many studies, however, have demonstrated the importance of a neuro-endocrine control of the efficiency of immune responses. It has been shown that the activation of the HPA axis, followed by the secretion of glucocorticoids, significantly lowers the efficiency of cytotoxic-mediated immune responses, thus affecting the development of anti-tumoral (Visintainer *et al.*, 1982) and anti-viral immunity (Koff & Dunegan, 1986; Hermann *et al.*, 1994). In various cases of viral (Hermann *et al.*, 1994; Dunn & Vickers, 1994; Sundar *et al.*, 1991) or bacterial infections (Gonzalo *et al.*, 1993), on the other hand, one has observed that macrophage-dependent and cytotoxic-mediated immune response induce glucocorticoid production by the neuroendocrine system. These results suggest the existence of a negative neuro-endocrine feedback on the immune response. Surprisingly, in some cases, one has found that this feedback has a positive effect on the survival of the organism and the elimination of the pathogen. In particular, one has observed in murine models that glucocorticoid production increases the resistance in cases of influenza virus infection (Hermann *et al.*, 1994) or bacterial toxic shock (Gonzalo *et al.*, 1993). The classical paradigm of the immune response which states that the strongest response is also the most efficient, does not account for the fact that this negative neuroendocrine feedback can have either a positive or a negative effect on pathogen elimination, nor for its advantages for the organism.

The explicit consideration, in our model, of the functional integrity of the organism (O), the HPA neuro-hormonal axis (H, k_h), as well as the injuries caused by the pathogen (α) and by the induced immune response (β) allows us to explore a wide range of host/pathogen dynamics.

In a first step, we have analysed the contributions of parameters k_p and k_i which quantify the proliferation rate of the pathogen and the sensitivity of the pathogen to the immune response, respectively. Starting from a healthy state, numerical simulations with different values of these parameters, allow to divide the parameter space into regions which lead preferentially to one of the four attractors of the system: the “zero state”, “pathogen death/organism alive”, “pathogen growth/organism death” and “chronic infection” [Fig. 6(a)].

In a second step, for a given set of k_p and k_i values allowing for chronic infection, we have explored the role of parameters k_r (pathogen immunogenicity) and k_h (activation of the HPA axis by the immune

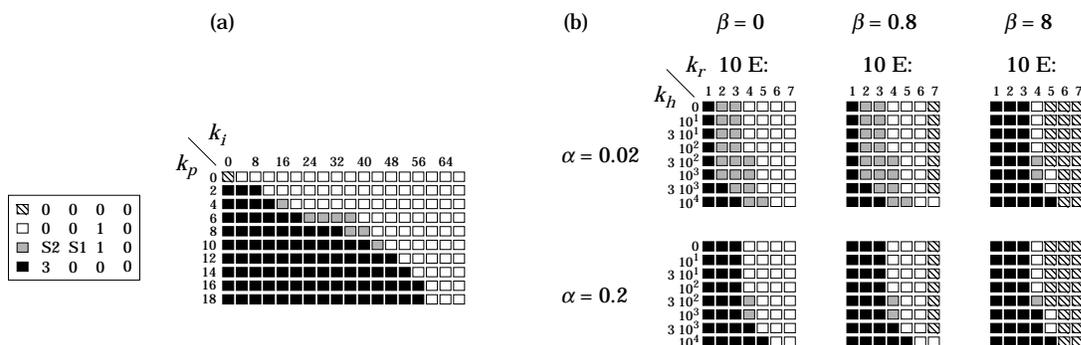


FIG. 6. Qualitative dynamics of eqns (1–4) upon pathogen encounter, starting from the initial conditions specified in Appendix C. The matrices give the final state that is reached by the system for different combinations of values of chosen couples of parameters (when parameter values are not specified, they are as in Appendix C). By comparing these different matrices, one can see how the parameters modify the region of attraction of the different regime states.

response), for different values of parameters α and β (the toxicities of the pathogen and of the immune response). For each couple of values of these latter parameters there is a range of k_r , and k_h , values which gives rise to the chronic attractor, in good agreement with the logical analysis which predicts that α and β are involved in the functionality of the positive loop **O** (see Appendix A). Moreover, one sees in Fig. 6(b), that when α and β increase, the domains of attraction of the different steady states are strongly modified in the parameter space k_r/k_h , with a progressive contraction of the “chronic infection” domain and expansion of the “pathogen growth/organism death” domain. In addition, as β increases, the “zero state” domain extends, which means that the pathogen is eliminated but the immune response itself causes organism death.

The effect of k_r , the pathogen immunogenicity, in relation with the neuro-endocrine control of the immune response is illustrated in Fig. 7 with some typical simulations. Depending on k_r , the issues of the host/pathogen conflicts can be classified into two main sets. In the first set ($k_r = 10^4$), at low k_h , the immune response is efficient enough to eliminate the pathogen without significant injury to the organism. Stronger neuro-endocrine feedback (i.e. increased k_h) results in a weakening of the efficiency of the immune response together with an increase of organism injuries by the pathogen which can lead to death. In a second set, characterized by higher k_r values ($k_r = 10^5$), the immune response is also able to eliminate the pathogen at low k_h , but the induced response destroys the organism as well. In this case, higher k_h values may lead to the preservation of the organism. However, if the HPA axis damps the immune response too strongly, the pathogen can no longer be eliminated and the system settles in the attractor “pathogen growth/organism death”. Note

that for high pathogen immunogenicity the system cannot sustain a stable chronic state as can be seen in Fig. 8 on the comparative bifurcation graphs for $k_r = 10^4$ and $k_r = 10^5$.

Our analysis thus suggests that the “optimal” immune response is not the response of maximum amplitude, but rather the response which consist in the best compromise between the elimination of the pathogen and the damages inflicted to the organism by direct or indirect destruction of tissues or organs caused by immune mediators.

Experimental data demonstrate the existence of a threshold for the activation of a neuro-endocrine feedback by immune mediators. It has indeed been shown that the HPA axis is induced by injections of high—and not by low—doses of antigen (Stenzel-Poore *et al.*, 1993). Such a threshold can be explained by the fact that the mediators of inflammatory responses, such as IL-1, need to reach a systemic level in order to trigger the synthesis of glucocorticoids. Below this threshold, the response remains local and harmless for the organism. Above this threshold, the response perturbs the integrity of the organism and is inhibited by the HPA axis. The notion of a response threshold for the activation of the HPA axis has been introduced in our model through the increasing sigmoid FA_2 in eqn (4). When the HPA axis is switched on, the results in this section suggest an additional distinction as a function of the immune response level. Indeed, activation of the neuro-endocrine feedback has positive consequences only when the amplitude of the response, which is a function of k_r , exceeds a certain level. At intermediate response levels, activation of the same negative feedback is unfavourable for resolving the host/pathogen conflicts. These results show that our model encompasses and clarifies the paradox of the neuro-endocrine feedback on the immune response.

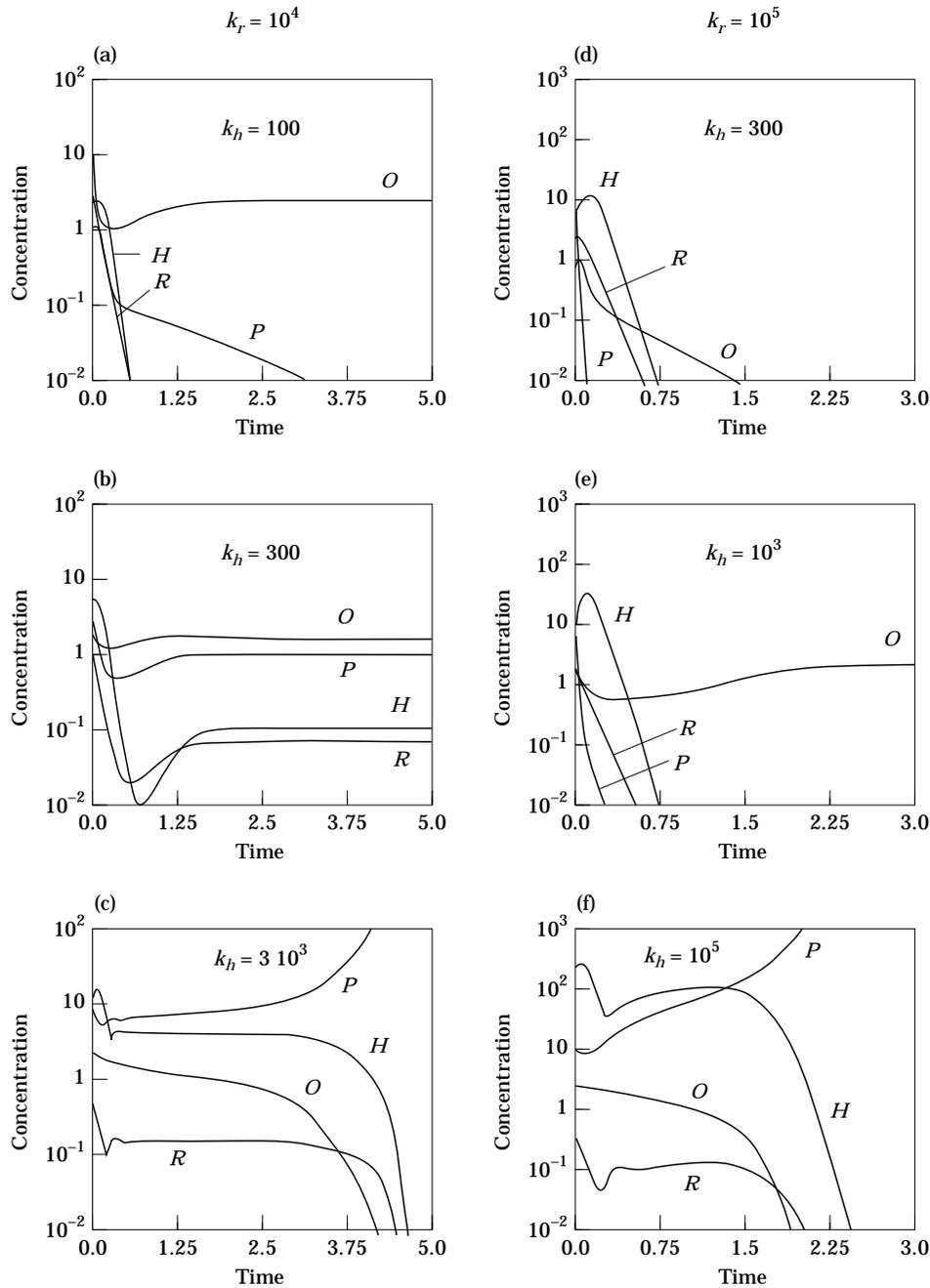


FIG. 7. Influence of pathogen immunogenicity and neuro-endocrine control of the immune response on the outcome of infections. The initial state and parameter values are specified in Appendix C. Left panel ($k_r = 10^4$): increasing the strength of the neuroendocrine feedback results in a weakening of the efficiency of the immune response and has a negative effect on pathogen elimination and organism health. Right panel ($k_r = 10^5$): increasing the strength of the neuroendocrine feedback has a positive influence on organism preservation by diminishing the toxic consequences of the immune response itself.

In the next two sections, we apply the preceding results in the study of stress-mediated immune regulation and toxic shock syndrome.

4.3.3. Stress and immune response

Surgical or psychological stress-induced psy-

choneural stimulation, via the HPA axis, activates the adrenal cortex to release glucocorticoids, which elicit various alterations of glucocorticoid-sensitive cell-mediated immunological processes in man and animals. Animals exposed to surgical or psychological stress showed a substantial decrease in Natural Killer cell

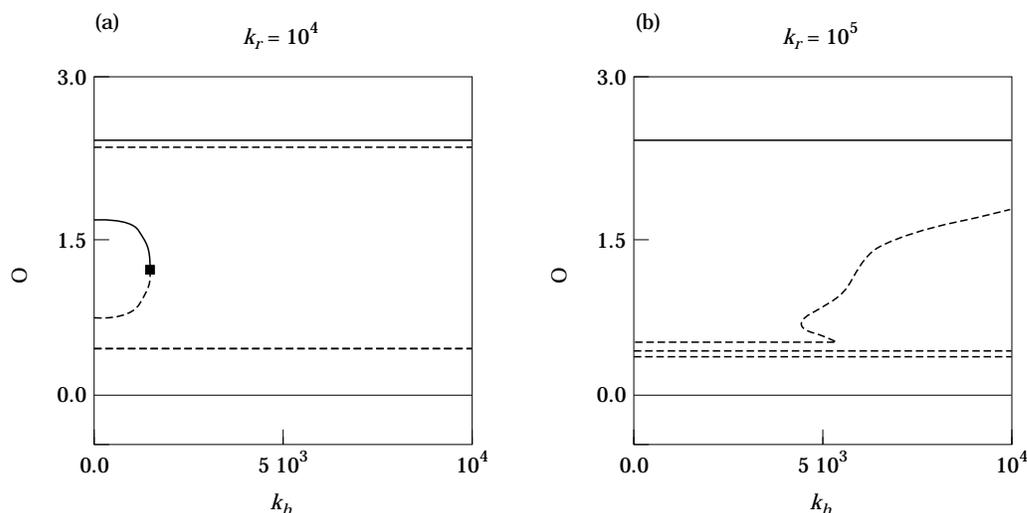


FIG. 8. Bifurcation graphs for different values of the pathogen immunogenicity, k_r . The steady states characterizing the health of the organism (O) are represented as a function of the strength of activation of the HPA axis, k_h . Other parameter values are given in Appendix C. Solid lines correspond to stable steady states, dashed lines to unstable ones. For high pathogen immunogenicity the system cannot sustain a stable chronic infection state.

cytotoxicity against tumor in *in vitro* assay (Pollock *et al.*, 1987; Ben-Eliyahu *et al.*, 1991) and multiple animal models demonstrate that stress reduces tumor rejection and decreases survival (Visintainer *et al.*, 1982). These findings support the hypothesis that stress can facilitate the metastatic process via suppression of the immune system. On the other hand, activation of the HPA axis by restraint stress or by the addition of glucocorticoid analogs increases the susceptibility of macrophages from mice to the *in vivo* growth of *Micobacterium avium* (Brown *et al.*, 1993). Recent observations provide evidence that psychological stress can also influence the anti-viral cellular immunity. For example, stress can induce an increase of the frequency and severity of recurrent herpes simplex (HSV) infections by the suppression of macrophage-mediated lysis of HSV infected cells (Koff *et al.*, 1986). In contrast, restraint stress has been associated with an enhanced probability of survival, attributable to elevated levels of circulating glucocorticoids, during influenza virus infection (Hermann *et al.*, 1994).

In our model, stress disturbances can be represented by the initial values of H . In Fig. 9, we have explored the dependence of the immune response on the initial value of H . Figure 9(a) summarizes the results of a set of simulations for different values of k_r and k_h . Depending on these initial values, the issues of the host/pathogen conflicts are modified. Figure 9(b) gives the trajectories in the phase plane (O , P) starting from a healthy organism and different pathogen doses, for two values of k_r , and initial values of H . These diagrams show a drastic

modification of the basins of attractions as a function k_r . For $k_r = 10^4$, an initial value $H = 0$ leads to “chronicity” or “pathogen death/organism recovery”, depending on the initial pathogen dose. For an initial value $H = 10$, the “chronic” attractor dominates. For $k_r = 10^5$, the “chronic” state is no longer a stable steady state. An initial value $H = 0$ leads to the “zero” attractor, whereas for an initial value $H = 10$, the immune response succeeds to eliminate the pathogen and leads to full recovery of the organism.

These variations of the initial value of H show that an initial stress can, in our model, influence the outcome of the host/pathogen conflict and that the resulting effect also depends on the immunogenicity of the pathogen. This leads us to suggest that in infections with a pathogenesis mostly imputable to the immune response, like the Dengue Shock Syndrome, Trypanosome Cerebral Malaria or hepatitis A and B, one could reach a more favourable issue if one activates the HPA axis, e.g. by stress induction or by using glucocorticoid analogs.

4.3.4. Toxic shock syndrome

Superantigens (SAGs) and lipopolysaccharide (LPS) constitute a new class of antigens that includes bacterial and viral antigens. If classical antigens have to be processed by antigen presenting cells, SAGs and LPS can stimulate the immune system in their native conformation. Bacterial SAGs and LPS are recognized as a major factor in the pathogenesis of bacterial septic shock induced by Gram-negative bacteria, a

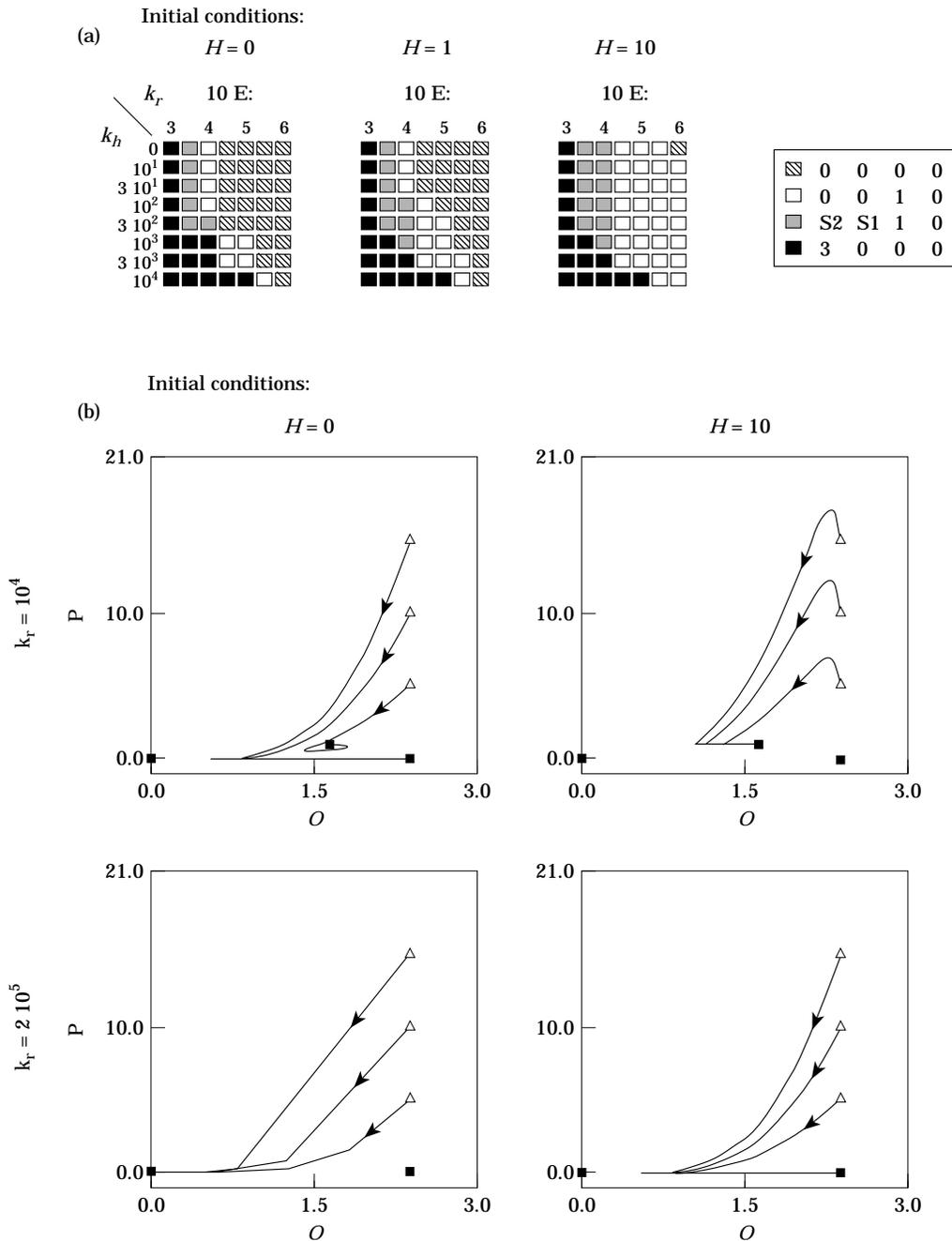


FIG. 9. Influence of stress on the issue of host/pathogen conflicts. (a) The three matrices correspond to different initial values of the neuroendocrine component of the system, H . Each box indicates the final regime state for a combination of values of k_r and k_h . (b) Representative trajectories in the plane (O, P) as a function of different initial values of H and of the pathogen dose, P . Two values of the couple k_r/k_h have been selected: $10^4/10^2$ and $2 \cdot 10^5/10^2$. Non-specified initial conditions and parameters values are given in Appendix C.

disease with significant mortality in humans. This is related to the property of SAGs to mediate rapid and massive activation of the immune system leading to systemic cytokine secretion. Pathologies related to SAGs and LPS are thus mostly attributed to the production of proinflammatory cytokines by the

immune response (Miethke *et al.*, 1992; Zuckerman *et al.*, 1989).

In our model, these antigenic profiles can be represented by $k_p = 0$ (SAGs or LPS do not proliferate), $ki = 0$ (the immune system does not eliminate SAGs or LPS) and $\alpha = 0$ (they are not toxic

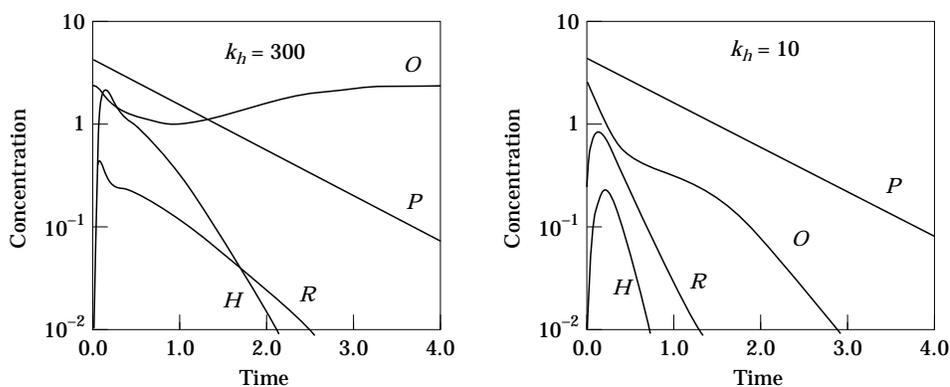


FIG. 10. Effect of the neutralisation of the HPA axis on SAGs or LPS administration. Time evolution for different values of k_h , the strength of activation of the HPA axis. The initial state corresponds to a healthy organism infected with a non proliferating pathogen (initial dose $P = 4$). Depending on the strength of the negative feedback of the HPA axis on the immune response, one observes the death ($k_h = 10$) or full recovery of the organism ($k_h = 300$). For these simulations $k_p = k_i = \alpha = 0$ and the other parameter values are as in Appendix C.

by themselves). For these parameter values, we have tested the influence of the inhibition of the HPA axis on SAGs or LPS administration. Figure 10 shows that neutralisation of the HPA axis ($k_h = 10$) enhances the lethal consequences of their administration. This result is in good agreement with experimental data showing that preliminary administration of glucocorticoid-antagonists sensitizes the organism to toxic shock (Gonzalo *et al.*, 1993).

5. Conclusions and Perspectives

The logical tool has been helpful to provide a qualitative picture of the behavior of our four-variable model (location and nature of the steady states, location of the separatrices, etc.), and has helped us to determine the corresponding elements in the differential context.

In the logical approach the relation between feedback loops and steady states is clearly understood (Thomas & D'Ari, 1990; Thomas *et al.*, 1995). Proceeding from the logical caricature to a differential model, the interdependency of the different loops has been increased and the relationship between loops and steady states weakened. Nevertheless, in the case of our four-variable system, we could still predict specific dynamical changes (loss of multistationarity or homeostasis) on the basis of the logical analysis.

From a biological point of view an essential aspect of our approach is to consider the physiological interaction between immunity and the neuroendocrine system, which results from a sharing of ligands and receptors. To this end, in addition to classical parameters such as pathogen growth, pathogen immunogenicity, efficiency of the immune response and damages inflicted by the pathogen to the organism, we have introduced variables and par-

ameters representing the viability of the organism, the toxicity of the immune response and its neurohormonal control. First, our model accounts, in terms of transitions among multiple attractors, for a large spectrum of classical and less classical immune responses. Second, it allows to redefine the notion of "optimal" immune response, to clarify the paradoxical effects of neuroendocrine inhibition of the response, and to suggest ways to modify the outcome of infections which usually lead to immunotoxicity.

In particular, our analysis suggests that the "optimal" immune response is not the response of maximum amplitude, but rather the response which consists in the best compromise between the elimination of the pathogen and the integrity of the organism. On the basis of our results, we propose that administration of glucocorticoid analogs or activation of the HPA axis by stress could advantageously modify the outcome of infections which are accompanied by immune toxicity.

In this study, we have considered the negative feedback on the immune response of the HPA axis. Several other negative feedbacks, such as the production of prostaglandins, IL-4, IL-10, IL-13 or TGF- β are well-documented and have also been shown to inhibit macrophage-dependent and cytotoxic-mediated immune responses. Unlike the induction of glucocorticoid synthesis, however, these feedbacks are produced locally in response to a local stress. The fact that the activation of the HPA axis requires a systemic level of immune mediators and that it can be triggered by an external stress endows this feedback with a particular integration capacity. On the basis of our results, we thus propose that the HPA axis constitutes a regulator of the amplitude of the immune response and of its potential toxicity.

Our model also leads to interpret superantigen (SAGs) and lipopolysaccharides (LPS)-induced immune responses. Since their discovery, SAGs and LPS constitute a source of immunological questioning. The expression of these highly immunogenic molecules does not fit into the "classical" escaping strategies of pathogens, which aim at a weakening of their immunogenicity e.g. by antigenic variation, production of immunosuppressive factors and functional inactivation/deletion of regulatory or effector cells, etc. However, the absence of sequence homology between the different groups of bacterial (*Staphylococcus aureus*, *Mycoplasma arthritidis*, *Clostridium perfringens*) or viral (Mouse Mammary Tumor Virus, Rabic Virus) SAGs suggest a coevolution leading to common functional properties and some evolutive advantage for the pathogen. In fact, it is now well established that, despite their high activatory properties, bacterial SAGs do not induce the differentiation of naive T helper cells into memory cells. After activation by SAGs, T helper undergo a phase of unresponsiveness called "anergy" (Migita & Ochi, 1993). Some authors have suggested that this immunosuppression could be the consequence of a massive activation of T cells by SAGs which could be followed by the production of immunosuppressive factors and lead to T cell anergy via a negative feedback. Induced by SAG injection and known as strong immunosuppressors, glucocorticoids are considered as possible mediators of this feedback (Gonzalo *et al.*, 1993).

Similarly, several studies suggest that LPS affect the ability of the immune system to respond to a potential or ongoing immune challenge (Grbic *et al.*, 1991). The detailed mechanism of LPS immunosuppression is still unknown. However, LPS injection induces glucocorticoid secretion (Zuckerman *et al.*, 1989) and it is described that LPS-induced stress modulate antigen presenting cells (APC) trafficking and distribution (Roake *et al.*, 1995).

In conclusion, the non-specific immunosuppression induced by SAGs, and possibly by LPS, could confer an evolutive advantage to the bacteria which produce these antigens and, according to our model predictions, be crucial for the survival of the host. Indeed, if this immunosuppression allows the pathogen to escape the immune response, it also lowers the damages inflicted to the organism by the same immune response. Thus, we suggest that these particular antigens could result from a host/pathogen coevolution and constitute an escaping mechanism to the immune response, thanks to the exploitation of the coupling between immune and neuro-endocrine systems.

Finally, it should be stressed that both our differential model and its logical caricature, are essentially a qualitative description of the biological problem investigated. The choice of variables with a wide physiological meaning and of the form of the functions describing the interactions aims at overcoming the lack of quantitative data and at drawing a robust qualitative picture of the regulatory network involved. In this context, our model analysis gives a coherent global picture of the neuro-hormonal regulation of the immune response. It leads to an interpretation of several experimental observations as well as to broad guidelines for experimentation, which could be further specified according to particular experimental models.

The induction of a specific immune response is determined by the activation of T CD4 lymphocytes. These CD4 T cells can be classified into TH1 and TH2 lines according to their cytokine release patterns and their regulatory functions [for a review, see Fitch *et al.* (1993)]. An important observation is that if TH1 responses are protective, then TH2 responses tend to be counter-protective and vice versa. Recent data also show that the activation of the HPA axis tends to decrease TH1 activity and to enhance TH2 activity [for a review see Rook *et al.* (1994)]. In the present modeling we focus mainly on antiviral and antibacterial immune responses which are essentially of the TH1-type. A next step will be to include in the model the differentiation of TH1 and TH2 cell sub-classes, taking into account that TH2 regulatory and effector cells are less toxic and less sensitive to inhibitory effects of glucocorticoids. This should allow to analyze the constraints imposed by toxicity and immunogenicity on the choice of the class of immune response. Furthermore, introduction of the TH1/TH2 dichotomy should also lead to investigate the impact of stress and neuroendocrine control on TH1 or TH2 mediated autoimmune diseases and TH2 mediated allergies. Indeed, several studies suggest a negative feedback of the HPA axis on TH1-type autoimmune reactions (Schauenstein *et al.*, 1987) and a positive feedback on allergic (TH2) reactions (McQueen *et al.*, 1989).

We thank R. Thomas for his careful reading of the manuscript and several useful suggestions. E. M. is supported by a Grant FRIA (Fond pour la Recherche Scientifique, dans l'Industrie et l'Agriculture, Belgium). D. T. is supported by a Grant FNRS-Télévie (Fonds National de la Recherche Scientifique, Belgium) and acknowledge financial support by the Fonds Van Buren and the Fonds Defay. M. K. acknowledges financial support by the Belgian Program on Interuniversity Attraction poles and by the Fonds National de la Recherche Scientifique

(Crédit aux Chercheurs). O. L. is Research Associate from the *Fonds National de la Recherche Scientifique* (Belgium). All simulations of differential systems have been made using GRIND, kindly provided by R. J. de Boer.

REFERENCES

- ANDO, K., MORIYAMA, T., GUIDOTTI, L. G., WIRTH, S., SCHREIBER, R. D., SCHLICHT, H. J., *et al.* (1993). Mechanism of class I restricted immunopathology. A transgenic mouse model of fulminant hepatitis. *J. Exp. Med.* **178**, 1541–1554.
- ANTIA, R. & KOELLA, J. C. (1994). A model of non-specific immunity. *J. theor. Biol.* **168**, 141–150.
- BEHN, U., VAN HEMMEN, J. L. & SULZER, B. (1993). Memory to antigenic challenge of the immune system: synergy of idiotypic interactions and memory B cells. *J. theor. Biol.* **165**, 1–25.
- BEN-ELIYAHU, S., YIRMIYA, R., LIEBESKIND, J. C., TAYLOR, A. N. & GALE, R. P. (1991). Stress increases metastatic spread of a mammary tumor in rats: evidence for mediation by the immune system. *Brain. Behav. immun.* **5**, 193–205.
- BOCHAROV, G. A. & ROMANYUKHA, A. A. (1994). Mathematical model of antiviral immune response III. Influenza A virus infection. *J. theor. Biol.* **167**, 323–360.
- BRASS, A., GRENCIS, R. K. & ELSE, K. J. (1994). A cellular automata model for helper T cell subset polarisation in chronic and acute infection. *J. theor. Biol.* **166**, 189–200.
- BROWN, D. H., SHERIDAN, J., PEARL, D. & ZWILLING, P. B. S. (1993). Regulation of mycobacterial growth by the hypothalamus-pituitary-adrenal axis: differential responses of *Mycobacterium bovis* BCG-resistant and susceptible mice. *Infect. Immun.* **61**, 4793–4800.
- DE BOER, R. J. & HOGEWEG, P. (1986). Interactions between macrophages and T-lymphocytes: tumor sneaking through intrinsic to helper T cell dynamics. *J. theor. Biol.* **120**, 331–351.
- DE BOER, R. J. & PERELSON, A. S. (1995). Towards a general function describing T cell proliferation. *J. theor. Biol.* **175**, 567–576.
- DE-KOSSODO, S. & GRAU, G. E. (1993). Profiles of cytokine production in relation with susceptibility to cerebral malaria. *J. Immunol.* **151**, 4811–4820.
- DOBBS, C. M., VASQUEZ, M., GLASER, R. & SHERIDAN, J. F. (1993). Mechanisms of stress-induced modulation of viral pathogenesis and immunity. *J. Neuroimmunol.* **48**, 151–160.
- DUNN A. J. & VICKERS, S. L. (1994). Neurochemical and neuroendocrine responses with Newcastle disease virus administration in mice. *Brain. Res.* **645**, 103–112.
- FISHMAN, M. A. & PERELSON, A. S. (1993). Modelling T cell-antigen presenting cell interactions. *J. theor. Biol.* **160**, 311–342.
- FISHMAN, M. A. & PERELSON, A. S. (1994). Th1/Th2 Cross-Regulation. *J. theor. Biol.* **170**, 25–56.
- FITCH, F. W., MCKISIC, M. D., LANCKI, D. W. & GAJEWSKI, T. F. (1993). Differential regulation of murine T lymphocyte subsets. *Annu. Rev. Immunol.* **11**, 29–48.
- FLEICHER, B., FLEICHER, S., MAIER, K., WIEDMANN, K. H., SACHER, M., THALER, H. & VALLBRACHT, A. (1990). Clonal analysis of infiltrating T lymphocytes in liver tissue in viral hepatitis A. *Immunology* **69**, 14–19.
- GONZALO, J. A., GONZALEZ-GARCIA, A., MARTINEZ-A, C. & KROEMER, G. (1993). Glucocorticoid-mediated control of the activation and clonal deletion of peripheral T cells in vivo. *J. Exp. Med.* **177**, 1239–1246.
- GRBIC, J. T., MANNICK, J. A., GOUGH, D. B. & RODRICK, M. L. (1991). The role of prostaglandin E2 in immune suppression following injury. *Ann. Surg.* **214**, 253–263.
- HERMANN, G., BECK, F. M., TOVAR, C. A., MALARKEY, W. B., ALLEN, C. & SHERIDAN, J. F. (1994). Stress-induced changes attributable to the sympathetic nervous system during experimental influenza viral infection in DBA/2 inbred mouse strain. *J. Neuroimmunol.* **53**, 173–180.
- KARUNAWEEERA, N. D., GRAU, G. E., GAMAGE, P., CARTER, R. & MENDIS, K. N. (1992). Dynamics of fever and serum levels of tumor necrosis factor are closely associated during clinical paroxysms in *Plasmodium vivax* malaria. *Proc. Natl. Acad. Sci. U.S.A.* **89**, 3200–3203.
- KOFF, W. C. & DUNEGAN, M. A. (1986). Neuroendocrine hormones suppress macrophage-mediated lysis of herpes simplex virus-infected cells. *J. Immunol.* **136**, 705–709.
- KUNICKA, J. E., TALLE, M. A., DENHARDT, G. H., BROWN, M., PRINCE, L. A. & GOLDSTEIN, G. (1993). Immunosuppression by glucocorticoids: inhibition of production of multiple lymphokines by in vivo administration of Dexamethasone. *Cell Immunology* **149**, 39–49.
- MARCHUK, G. I., PETROV, R. V., ROMANYUKHA, A. A. & BOCHAROV, G. A. (1991). Mathematical model of antiviral immune response. I. Data analysis, generalized picture construction and parameters evaluation for hepatitis B. *J. theor. Biol.* **151**, 1–40.
- MCLEAN, A. R. & NOWAK, M. A. (1991). Models of interactions between HIV and other pathogens. *J. theor. Biol.* **155**, 69–102.
- MCQUEEN, G. M., MARSHALL, J., PERDUE, M., SIEGEL, S. & BIENENSTOCK, J. (1989). Pavlovian conditioning of rat mucosal mast cells to secrete rat mast cell protease II. *Science* **243**, 83–85.
- MIETHKE, T., WAHL, C., HEEG, K., ECHTENACHER, B., KRAMMER, P. H. & WAGNER H. (1992). T cell-mediated lethal shock triggered in mice by the superantigen *Staphylococcus aureus* enterotoxine B: critical role of tumor necrosis factor. *J. Exp. Med.* **175**, 91–98.
- MIGITA, K. & OCHI, A. (1993). The fate of anergic T cells in vivo. *J. Immunol.* **150**, 763–770.
- POLLOCK, R. E., LOTZOVA, E., STANFORD, S. D. & ROMSDAHL, M. M. (1987). Effect of surgical stress on murine natural killer cell cytotoxicity. *J. Immunol.* **138**, 171–178.
- ROAKE, J. A., RAO, A. S., MORRIS, P. J., LARSEN, C. P., HANKINS, D. F. & AUSTYN, J. M. (1995). Dendritic cell loss from nonlymphoid tissues after systemic administration of lipopolysaccharide, tumor necrosis factor, and interleukin 1. *J. Exp. Med.* **181**, 2237–2247.
- ROOK, G. A., HERNANDEZ-PANDO, R. & LIGHTMAN. (1994). Hormones, peripherally activated prohormones and regulation of the Th1/Th2 balance. *Immunology Today* **15**, 301–303.
- SAPOLSKY, R., RIVIER, C., YAMAMOTO, G., PLOTSKY, P. & VALE, W. (1987). Interleukin-1 stimulates the secretion of Hypothalamic Corticotropin-Releasing Factor. *Science* **233**, 522–524.
- SCHAUENSTEIN, K., FASSLER, R., DIETRICH, H., SCHWARTZ, S., KROEMER, G. & WICK, G. (1982). Disturbed immune-endocrine communication in autoimmune disease. Lack of corticosterone response to immune signals in obese strain chickens with spontaneous autoimmune thyroiditis. *J. Immunol.* **139**, 1830–1833.
- SCHWEITZER, N. & ANDERSON, R. (1991). Helminths, immunology and equations. *Immunol. Today* **12**, A76–A81.
- SEGEL, L. A. & JÄGER, E. (1994). Reverse engineering: a model for T-cell vaccination. *Bull. Math. Biol.* **56**, 687–721.
- SEGEL, L. A., JÄGER, E., ELIAS, D. & COHEN, I. R. (1994). A quantitative model for autoimmune disease and T-cell vaccination: does more mean less? *Immunology Today* **16**, 80–84.
- SNOUSS, E. H. & THOMAS, R. (1993). Logical identification of all steady states: the concept of feedback loop-characteristic states. *Bull. Math. Biol.* **55**, 973–991.
- STENZEL-POORE, M., VALE, W. W. & RIVIER, C. (1993). Relationship between antigen-induced immune stimulation and activation of the hypothalamic-pituitary-adrenal axis in the rat. *Endocrinology* **132**, 1313–1318.
- SUNDAR, S. K., CIERPIAL, M. A., KAMARAJU, L. S., LONG, S., HSIEH, S., LORENZ, C., *et al.* (1991). Human immunodeficiency virus glycoprotein (gp120) infused into rat brain induces interleukin 1

- to elevate pituitary-adrenal activity and decrease peripheral cellular immune responses. *Proc. Natl. Acad. Sci. U.S.A.* **88**, 11246–11250.
- THIEFFRY, D., COLET, M. & THOMAS, R. (1993). Formalization of regulatory networks: A logical method and its automatization. *Math. Modelling Sci. Computing.* **2**, 144–151.
- THOMAS, R. & D'ARI, R. (1990). *Biological Feedback*. Boca-Raton, Florida: CRC-Press.
- THOMAS, R. (1991). Regulatory networks seen as asynchronous automata: a logical description. *J. theor. Biol.* **153**, 1–23.
- THOMAS, R., THIEFFRY, D. & KAUFMAN, M. (1995). Dynamical behaviour of biological regulatory networks. I. Biological role of feedback loops and practical use of the concept of the loop-characteristic state. *Bull. Math. Biol.* **57**, 247–276.
- TITUS, R. G., SHERRY, B. & CERAMI, A. (1991). The involvement of TNF, IL-1 and IL-6 in the immune response to protozoan parasites. *Immunoparasitology Today* **12**, A13 – A16.
- VISINTAINER, M. A., VOLPICELLI, J. R. & SELIGMAN, M. E. (1982). Tumor rejection in rats after inescapable or escapable shock. *Science* **216**, 437–439.
- ZUCKERMAN, S. H., SHELLHASS, J. & BUTLER, L. D. (1989). Differential regulation of lipopolysaccharide-induced interleukin 1 and tumor necrosis factor synthesis: effects of endogenous and exogenous glucocorticoids and the role of pituitary-adrenal axis. *Eur. J. Immunol.* **19**, 301–305.

APPENDIX A

Logical Analysis

The salient features of the logical formalism developed by R. Thomas and collaborators are:

- the use of logical variables (labelled x_i) and functions (labelled X_i) which can take two or more integer values (0, 1, 2, etc.);
- the introduction of specific logical values (labelled $s^{(1)}, s^{(2)}$, etc.) to represent threshold values;
- the introduction of logical parameters associated to each interaction (labelled K_{ij}) or set of interactions (labelled $K_{ijk} \dots$) exerted on a same element; these logical parameters take the values (0, 1, etc.) according to the logical scale of the corresponding variable;
- the consideration of asynchronous transitions for the variable values.

From the matrix of interactions, one can construct a state table of the system which gives, for each combination of values of the logical variables (“state vector”), the value of the corresponding logical functions (“image vector”). This table (not shown here) is then used both to localize the steady states of the system and to check the functionality of the different feedback loops. Here we summarize the main results of the logical analysis of our model. More details about the formalism can be found in Thomas, 1991 and Thomas *et al.*, 1995.

Upon inspection of the graph or matrix of interactions (Fig. 2) one can localise six feedback loops:

- three positive loops, labelled **P**, **O** and **POR**;
- three negative loops, labelled **PR**, **PO** and **RH**, respectively.

Using a computer program, one can then determine the parameter constraints for having each of these feedback loops functional in a given region of the variable space (see Thieffry *et al.*, 1993). These sets of parameter constraints are given in the Table A1. Note that, in order for several loops to be functional together, one just needs to fulfil the corresponding sets of parameter constraints together.

In the last row of Table A1, we give the set of constraints that has been chosen to guide our analysis of the differential model. For these parameter values, all six loops of the system are functional at least in part of the variable space. Together, these loops generate seven “singular” steady states (i.e. states located on one or more thresholds): $[s^{(1)}000]$, $[s^{(1)}010]$, $[00s^{(1)}0]$, $[s^{(2)}s^{(1)}10]$, $[s^{(3)}s^{(1)}s^{(1)}0]$, $[s^{(1)}0s^{(1)}0]$ and $[s^{(2)}s^{(1)}s^{(1)}0]$.

In addition to these “singular” steady states, the system has also three “regular” steady states (i.e. states with integer values): $[0000]$, $[0010]$ and $[3000]$. These regular steady states are simply the states for which the state vector and the image vector are identical in the state table (not shown here).

As seen in Table A1, parameter $K_{1,2}$ is involved in the functionality of the positive loop **P** only. Changing the value of this parameter therefore only affects the multistationarity generated by this positive loop. Similarly, parameter $K_{4,2}$ is only involved in the functionality of the negative loop **RH**. Thus, changing the value of this parameter only modifies the homeostatic property generated by this negative loop. The effect of the variation of the corresponding differential parameters, k_i and k_h , respectively, is presented in Section 4.2. Table A1 also shows that all other logical parameters are involved in the functionality of more than one loop.

APPENDIX B

Steady State Solutions of the Differential System (1–4)

The steady-state solutions of eqn (1) are:

$$P = 0 \quad (\text{B.1})$$

$$P = \frac{1 + k_i R}{k_p - (1 + k_i R)} \quad (\text{B.2})$$

The requirement of positive values for the pathogen level P imposes restrictions on the parameter values.

TABLE A1
Parameter constraints for the functionality of the different feedback loops of the system

Loop	Sign	Domain	K_1	$K_{1,1}$	$K_{1,2}$	K_2	$K_{2,1}$	$K_{2,2}$	$K_{2,3}$	$K_{2,4}$	$K_{2,13}$	$K_{2,14}$	$K_{2,34}$	K_5	$K_{5,1}$	$K_{5,2}$	$K_{5,3}$	$K_{5,12}$	$K_{5,13}$	$K_{5,23}$	$K_{5,123}$	K_4	$K_{4,2}$
P	+	$s^{(1)}[12][0][1]$	[0]	[123]	[123]																		
		$s^{(1)}[0][01][01]$	[0]	[123]	[123]																		
O	+	$[3][2]s^{(1)}[01]$																					
		$[3][01]s^{(1)}[01]$																					
PR		$[0]2[2]s^{(1)}[01]$																					
		$[0]2[01]s^{(1)}[01]$																					
	-	$s^{(2)}s^{(1)}[1][1]$	[01]	[01]	[23]	[0]	[12]																
		$s^{(2)}s^{(1)}[1][0]$	[01]	[01]	[23]	[0]	[12]																
RO		$s^{(2)}s^{(1)}[0][1]$	[01]	[01]	[23]	[0]	[12]																
		$s^{(2)}s^{(1)}[0][0]$	[01]	[01]	[23]	[0]	[12]																
		$s^{(2)}s^{(1)}[0][0]$	[01]	[01]	[23]	[0]	[12]																
		$[3]s^{(2)}s^{(1)}[1]$	[01]	[01]	[23]	[01]	[2]																
		$[3]s^{(2)}s^{(1)}[0]$	[01]	[01]	[23]	[01]	[01]																
		$[2]s^{(2)}s^{(1)}[1]$	[01]	[01]	[23]	[01]	[2]																
RH		$[0]1s^{(2)}s^{(1)}[1]$	[01]	[01]	[23]	[01]	[2]																
		$[0]1s^{(2)}s^{(1)}[0]$	[01]	[01]	[23]	[01]	[01]																
		$[23]s^{(2)}[1]s^{(1)}$	[01]	[01]	[23]	[01]	[01]																
		$[23]s^{(2)}[0]s^{(1)}$	[01]	[01]	[23]	[01]	[01]																
		$[0]1s^{(2)}[1]s^{(1)}$	[01]	[01]	[23]	[01]	[01]																
		$[0]1s^{(2)}[0]s^{(1)}$	[01]	[01]	[23]	[01]	[01]																
POR	+	$s^{(3)}s^{(1)}s^{(1)}[1]$	[012]	[012]	[3]	[0]	[12]																
		$s^{(3)}s^{(1)}s^{(1)}[0]$	[012]	[012]	[3]	[0]	[12]																
Parameter values chosen			[0]	[0]	[3]	[0]	[0]	[0]	[0]	[0]	[0]	[0]	[0]	[0]	[0]	[0]	[0]	[0]	[0]	[0]	[0]	[0]	[1]

In this table, the subscripts 1, 2, 3 and 4 of the logical parameters K refer to P , R , O , and H , respectively. In the first column, the different loops of the system are indicated. The second column gives the corresponding sign of the loops. In the third column, the region of the variable space in which a loop is functional is specified. The other columns contain the corresponding constraints on the different logical parameters of the system. If there are no logical values specified there are no constraints on the value of the corresponding logical parameter. In the first row, the logical parameter K_1 represents the level of expression of P in the absence of all positive and in the presence of all negative contributions exerted on P ; $K_{1,1}$ represents the level of expression of P in the presence of the positive contribution of P on itself; $K_{1,12}$ represents the level of expression of P in the presence of the positive contribution of P and in the absence of the negative effect of R ; etc. In the second row, [0] and [123] mean that, in order to have the positive loop P functional in the domain $s^{(1)}[12][0][1]$, (i.e. $R = 1$ or 2 , $O = 0$ or 1 , $H = 0$ or 1), the corresponding parameters must take the values 0 and 1, 2 or 3, respectively. The last row gives the set of parameter values used to guide the analysis of the differential model. One can easily check that for these parameter constraints, all six feedback loops of the system are functional at least in a part of the variable space.

STEADY STATES IN THE ABSENCE OF PATHOGEN

$$(P = 0, B1)$$

The steady state solutions of eqns (2-4) corresponding to $P = 0$ are:

$$R = H = 0$$

$$O = 0 \text{ and } O = \frac{1}{2} \left\{ \frac{k_o}{d_o} \pm \sqrt{\left(\frac{k_o}{d_o}\right)^2 - 4} \right\}.$$

Provided $k_o/d_o > 2$ there are thus three steady state solutions for O of which the two outer are stable steady states.

STEADY STATES IN THE PRESENCE OF PATHOGEN

$$(P \neq 0, B2)$$

(a) for $O = 0$ and $k_p > 1$, there is an additional steady state in which:

$$R = H = 0 \text{ and } P = \frac{1}{k_p - 1}.$$

This steady state is unstable in the P direction.

(b) for $O \neq 0$: eqns (2) and (3) may be rewritten in the form:

$$\frac{O^2}{1 + O^2} = f(R) \text{ and } \frac{O^2}{1 + O^2} = O g(R)$$

where

$$f(R) = \frac{d_r(s^2 + P^2)(1 + H^2)}{k_r P^2} R$$

and

$$g(R) = \frac{(d_o + \alpha P + \beta R)}{k_o}$$

with P given by (B2) and

$$H = \frac{k_h R^2}{d_h(1 + R^2)}.$$

The steady-state solution for O is then given by:

$$O = \frac{f(R)}{g(R)} \tag{B.3}$$

where R satisfies the equation:

$$g^2 = f(1 - f) \tag{B.4}$$

Real positive values for O require that $0 < f < 1$ and $0 < g \leq \frac{1}{2}$.

Equation (B.4) is a polynomial of the 16th degree in R , which has to be solved numerically. However, the number and approximate location of the steady state values of R , as a function of the parameters of the system, can also be determined graphically from the intersections of g^2 and $f(1 - f)$. This leads to two to four additional (non zero) steady state values of R , and hence of the other variables of the system, as illustrated in Fig. B1 for two different values of parameter k_h .

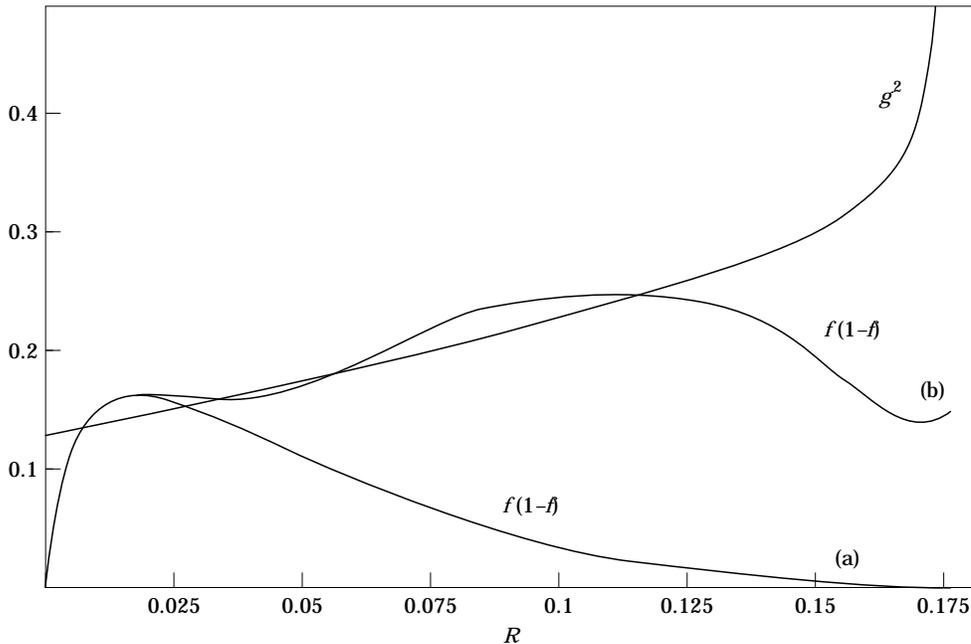


FIG. B1. Graphical analysis of the steady solutions. The intersections of g^2 and $f(1 - f)$ give the non-zero steady-state values of R . The parameter values are as in Appendix C, except for $s = 10$, $k_r = 10^3$. (a) $k_h = 0$ and (b) $k_h = 5000$.

APPENDIX C

Parameter Values

The composite parameters in eqns (1–4) are given by:

$$k_p = k'_p/d_p, \quad k_r = k'_r/d_p s_r, \quad k_o = k'_o/d_p s_o, \quad k_h = k'_h/d_p s_h$$

$$k_i = k'_i s_r/d_p, \quad s = s_{p2}/s_{p1}$$

$$d_r = d'_r/d_p, \quad d_o = d'_o/d_p, \quad d_h = d'_h/d_p$$

$$\alpha = \alpha' s_{p1}/d_p \text{ and } \beta = \beta' s_r/d_p$$

where the primes refer to the initial parameters. $1/d_p$

is the pathogen half-life time. s_r , s_o and s_h are, respectively, the threshold of action of variables R , O and H in their corresponding sigmoid (Hill) function. s_{p1} denotes the threshold for exponential growth of the pathogen and s_{p2} its threshold level for the activation of the immune response, with $s_{p1} < s_{p2}$. Unless otherwise specified, the numerical analysis and simulations were performed with the parameter values: $s = 100$, $d_r = 10$, $d_o = 2.5$, $d_h = 15$, $k_p = 7$, $k_r = 10^4$, $k_o = 7$, $k_h = 300$, $k_i = 34$, $\alpha = 0.02$, $\beta = 8$, and the initial conditions corresponding to an healthy organism ($R = 0$, $O = 2.379$, $H = 0$) infected with the pathogen dose $P = 10$.